SAND2021-12020C

Diesel Generator Model Development and Validation using Moving Horizon Estimation

Manisha Rauniyar†, Niranjan Bhujel, Timothy M. Hansen, Robert Fourney, Hossein Moradi Rekabdarkolaee, and Reinaldo Tonkoski
South Dakota State University
Brookings, South Dakota, USA
Email: †manisha.rauniyar@jacks.sdstate.edu

Phylicia Cicilio and Mariko Shirazi
University of Alaska Fairbanks
Fairbanks, Alaska, USA

Ujjwol Tamrakar
Sandia National Laboratories
Albuquerque, New Mexico, USA

***Abstract*—Diesel hybrid power systems including inverter-based generation have faster and more stochastic dynamics than traditional systems. It is necessary to develop accurate models of the system components to ensure the stability of these systems and proper controller design. The parameters of the diesel generators in hybrid power systems, such as the inertia constant, are time-varying, requiring online parameter estimation techniques. This paper presents a simplified linear model developed to represent the frequency dynamics of the detailed diesel generator system and validated the model using a moving horizon estimation (MHE) approach. The proposed optimization-based MHE algorithm is employed to accurately provide an estimation of multiple parameters of a simplified diesel generator model. The proposed method extracts the parameters minimizing a cost function with a given set of constraints on the parameters. A non-intrusive square wave excitation signal generated by step changes in load is used to perturb the system with minimal impacts on power system operation. MHE estimates the parameters based on the power and frequency from the diesel generator system measured using the phase-locked loop (PLL) and provides reasonable estimates of unknown parameters. The estimated parameters are further verified by using them back in the simplified model and comparing them with the PLL measurements to represent the frequency dynamics of the diesel genset system.**

***Index Terms*—diesel generator, measurements, noise, system dynamics, parameter estimation, moving horizon estimation.**

I. Introduction

In remote communities, distributed diesel generators (DGs) are usually the primary source of electric energy due to their low investment cost [1] (e.g., more than 300 remote communities in Canada [2] and Alaska [3]). Diesel generators can be integrated with renewable inverter-based generation, such as photovoltaic and wind, in such remote microgrids to reduce the reliance on imported diesel fuel and energy price. Inverter-based generation introduces faster and more stochastic dynamics compared to synchronous generation [4]. Thus, it becomes crucial to understand the dynamic response of diesel-backed microgrids for the accurate modeling of power system components. The parameters in these microgrids are time-varying; it becomes equally important to implement an online estimation technique for ensuring system stability and proper controller design.

A number of model parameter estimation techniques for generator plant model validation have been proposed for power system dynamic studies. The parameters of a generic large hydro generator have been derived from offline data based on the transient response field tests of the generator [5]. A practical approach in model selection and parameter estimation of a dynamic model representing gas power plants was developed via system identification methods based on field data that are further tuned using an iterative Cuckoo algorithm in [6]. However, these heuristic techniques are mainly applicable for extracting the non-time-varying parameters [7]. Offline tests are also costly due to time not-in-service, and are therefore less feasible due to cost and applicability for a small-scale DG operating as the primary or backup source of power in isolated microgrids.

An online approach has been developed for inertia and damping constant estimation of power plants based on the frequency measurements from phasor measurement units (PMUs) using the swing equation [8]. However, PMU measurements may not be readily available in microgrids. Extended and ensemble Kalman filters were used for parameter estimation in [9], where parameters are included in the state vector. However, the extended Kalman filter approaches are reliable only on linear systems and less accurate in case of non-linear dynamical systems as they use a first-order approximation of non-linear dynamic equations. Unscented Kalman filters have been used to estimate the states and parameters of a non-linear system with reasonable accuracy [10]. However, these Kalman filters assume that the noise is Gaussian which means Kalman filters may fail for non-Gaussian noise [11]. Moving horizon estimation (MHE) is likely to outperform Kalman filters for

This work is supported by the U.S. Department of Energy Office of Science, Office of Electricity Microgrid RD Program, and Office of Energy Efficiency and Renewable Energy Solar Energy Technology Office under the EPSCoR grant number DE-SC0020281.

The work at Sandia (Ujjwol Tamrakar) is supported by the US Department of Energy Office, Office of Electricity, Energy Storage Program.

Sandia National Laboratories is a multi-mission laboratory managed and operated by National Technology and Engineering Solutions of Sandia, LLC., a wholly owned subsidiary of Honeywell International, Inc., for the U.S. Department of Energy National Nuclear Security Administration under contract DE-NA-0003525. This paper describes objective technical results and analysis. Any subjective views or opinions that might be expressed in the paper do not necessarily represent the views of the U.S. Department of Energy or the United States Government.

similar computational cost [12].

MHE is an online optimization-based algorithm that is appropriate for estimating the parameters in microgrids to provide adaptive system protection and control. In [13], inertia and damping constants of synchronous machine were estimated using the MHE approach. The models used inside MHE in [13], [14] have partial knowledge of the parameters, where MHE provided the estimates of unknown parameters based on the knowledge of system input, system equations, and known parameters.

In this paper, a simplified state-space model is developed to simulate the frequency dynamics of detailed diesel generator system. MHE is employed to provide online estimations of an unknown set of parameters of the simplified DG and governor model based on frequency and electrical power. The frequency response is observed with obtained set of parameter estimates in the simplified linear model which was found to be very close to the detailed DG system. State and parameter estimation using the proposed method will have a wide range of applications in fast frequency control, stability analysis, and controller design purpose.

The paper is organized as follows: Section II introduces the system dynamics of the given diesel genset Simulink model. Section III describes the MHE approach employed for the parameter identification process followed by MHE formulation and implementation. The detailed simulation setup is described in Section IV. The estimates of MHE along with the validation results of the approach are presented and analyzed in Section V, and the paper is concluded in Section VI.

II. Simplified Dynamics of Governor-Generator System

The simplified block diagram of the DG system under study is shown in Fig. 1. The system contains a synchronous generator and an isochronous governor that provides an approximate model to represent the frequency dynamics of detailed diesel plant. Exciters and voltage regulators have significantly faster response than the frequency dynamics [15], thus the excitation system dynamics are neglected in this work. The simplified governor is represented by a single time-constant (T_g), which is shown to be adequately equivalent to the detailed governor response. With the assumptions made on deriving the approximated model used inside MHE, the estimator reduces the computational cost and provides quick convergence. Additionally, it is important to note that this simplified model is only used as the state equation for the MHE, whereas the actual simulations are carried out in a detailed model of the diesel genset as described in Section IV. The dynamics of the system are modeled using the swing equation and a differential equation representing engine-governor dynamics. Generator dynamics are represented by the following differential equation:

$$M\Delta\dot{\omega} + D\Delta\omega = \Delta P_m - \Delta P_e \tag{1}$$

where M and D represent the inertia constant and damping coefficient of the generator, respectively. $\Delta\omega$ is the change in system frequency, $\Delta\dot{\omega}$ represents the rate of change of frequency (ROCOF), ΔP_m is the change in the total mechanical power, and ΔP_e is the change in the total electrical power of the diesel genset system.

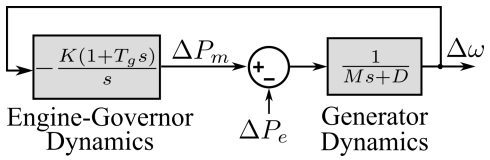

Fig. 1. Block diagram of the simplified model of the engine-governor-generator frequency dynamics.

In this paper the engine-governor dynamics are represented by the following differential equations:

$$\Delta\dot{P}_m = -K\Delta\omega - KT_g\Delta\dot{\omega} \tag{2}$$

$$\Delta\dot{z} = -K\Delta\omega \tag{3}$$

where $\Delta z = \Delta P_m + KT_g\Delta\omega$, and K and T_g represents the governor gain and equivalent time constant, respectively. We chose Δz as one of the states to simplify the state equations. Because we will only measure $\Delta\omega$, we are free to choose other states. Equations (1) and (3) can be combined and written in state-space form as:

$$\frac{d}{dt}\begin{bmatrix}\Delta z\\ \Delta\omega\end{bmatrix} = \begin{bmatrix}0 & -K\\ \frac{1}{M} & -(\frac{D}{M}+\frac{KT_g}{M})\end{bmatrix}\begin{bmatrix}\Delta z\\ \Delta\omega\end{bmatrix} + \begin{bmatrix}0\\ -\frac{1}{M}\end{bmatrix}\Delta P_e \tag{4}$$

Equation (4) contains four parameters. However, to represent the dynamics, we need to estimate the coefficients of the state-space model. Thus, Equation (4) can be written as:

$$\frac{d}{dt}\begin{bmatrix}\Delta z\\ \Delta\omega\end{bmatrix} = \begin{bmatrix}0 & -a_{12}\\ a_{21} & -a_{22}\end{bmatrix}\begin{bmatrix}\Delta z\\ \Delta\omega\end{bmatrix} + \begin{bmatrix}0\\ -a_{21}\end{bmatrix}\Delta P_e \tag{5}$$

where $a_{12} = K$, $a_{21} = 1/M$ and $a_{22} = (\frac{D}{M} + \frac{KT_g}{M})$. Equation (5) has only three coefficients which shows the same dynamics as represented by (4). Equation (4) is in the form of

$$\dot{x} = Ax + Bu \tag{6}$$

where $x = [\Delta z_k, \Delta\omega_k]^\top$ is the state and $u = \Delta P_e$ is the system input. The set of parameters $\{a_{12}, a_{21}, a_{22}\}$ will be estimated using MHE.

III. MHE Formulation and Implementation

Equation (5) can be converted to discrete-time, and the resulting output equation can be represented as:

$$x_{k+1} = A_d x_k + B_d u_k \tag{7a}$$

$$y_k = C_d x_k + v_k \tag{7b}$$

where $x_k = [\Delta z_k, \Delta\omega_k]^\top$ represents the state, $y_k = \Delta\omega_k$ represents the measurement, and $u_k = \Delta P_e$ represents the input to the system at discrete time instant k. Matrices A_d and B_d are state and input matrices, respectively. Because we are only measuring $\Delta\omega_k$, the output matrix can be written as $C_d = [0\ 1]$. The measurement noise v_k at a particular instant is unknown; however, information about the noise statistics

is known. MHE is able to give an estimate for different measurement noise distribution (both Gaussian [14] and non Gaussian). In this work, we are performing the simulation assuming non-Gaussian noise with zero mean and known covariance R.

Let $\mathcal{H}$ represent the set of discrete-time instant $\{q-L+1, q-L+2, ..., q\}$ where L is the backward horizon length, and q represent the current discrete instant. Let $\mathcal{P} = [a_{12}, a_{21}, a_{22}]^\top$ represent the vector of parameters to be estimated. Then, the MHE problem can be formulated as [16]:

$$\min_{\hat{x}_k, \hat{u}_k, \mathcal{P}} J_H = \sum_{k=q-L+1}^{q} ||y_k - C_d \hat{x}_k||_V^2 + \sum_{k=q-L+1}^{q-1} ||u_k - \hat{u}_k||_W^2 \quad (8a)$$

subject to

$$\hat{x}_{k+1} = A_d \hat{x}_k + B_d \hat{u}_k \quad \forall\ k \in \mathcal{H} - \{q\} \quad (8b)$$

$$\mathcal{P}_{min} \leq \mathcal{P} \leq \mathcal{P}_{max} \quad (8c)$$

where $||a||_A^2 = a^\top A a$ is the norm of vector a with respect to matrix A, and $\mathcal{P}_{min}$ and $\mathcal{P}_{max}$ represent vectors of minimum and maximum possible value of parameters, respectively. J_H in (8a) represents the cost function. The first term in the cost function is the measurement term that represents the difference between measured and estimated y. The weight of the first term is $V = R^{-1}$ [17], which depends upon noise covariance. Higher measurement noise corresponds to higher noise covariance and lower measurement weights, and vice-versa. The second term represents the actuation error as the difference between measured and estimated input. This difference arises because of the random disturbance. The effective value of the input signal would be the applied excitation signal with added random disturbance. Additionally, the system generating the excitation signal could contain error. The second term corresponds to this error and is termed process noise. The weight for the second term W is the inverse of process noise covariance. We are not considering process noise, thus we will choose a value of $W >> V$. The first constraint (8b) represents the discrete-time state equation, and the second constraint (8c) limits the parameters to reasonable limits based on domain knowledge. Based on the domain knowledge from [15], the constraint limit on the parameters have been set to a maximum of 100 and a minimum of 0 in the given system. It provides the parameter estimates within realistic range of values. Although the state equation is linear with respect to the states, the above optimization problem is non-linear because matrices A_d and B_d contains parameters that are decision variables.

The MHE is implemented using CasADi — an open-source optimization package for MATLAB [18]. When new estimates are required, the system is excited by a square wave excitation signal generated by step changes in load. A square wave was selected because our preliminary analyses related to frequency dynamics showed a smaller estimation error compared to other signals [14]. The selection of sample time comes from the smallest time constant of the system calculated using eigenvalues of the state matrix A. At every sampling instant, new measurements are taken and appended to the data set, while the oldest measurement data are discarded. The above-formulated optimization problem is then solved online at every sampling instant giving the estimation of parameters and states over the horizon length. The solution from the previous sample instant is used as an initial guess for the solver, which reduces the number of iterations and, hence, computation time. The state differential equations are discretized using *Runge-Kutta* method of order 4.

IV. Simulation Setup

MHE was used to estimate the parameters (a_{12},a_{21}, a_{22}) of the detailed simulation setup of the diesel genset shown in Fig. 2. The estimation process was conducted on a linearized model with an unknown set of parameters to test the validity of the MHE approach. The detailed DG models of the governor and synchronous machine were used from the standard library in MATLAB/Simulink. The MATLAB model was simulated with a 400 kVA, 480 V diesel-genset using the standard synchronous generator model for a 406 kVA, 460 V, 60 Hz machine [19], the DEGOV model for the governor [20] based on implementation in [21], and the DC4B model for the exciter [22] as described in [23]. This work has compiled parameter values for the governor and exciter from several sources to create parameter values for the benchmark governor [7], [20] and exciter [22], [24]. The parameter values implemented in the benchmark models are outlined in Table I.

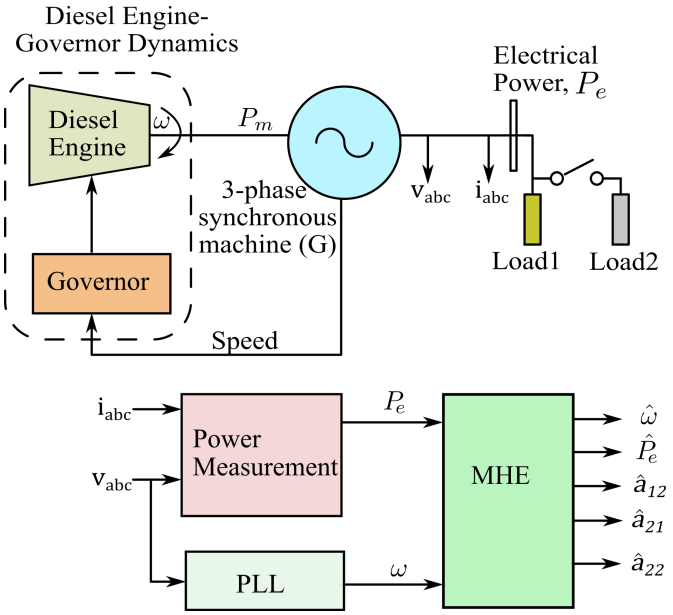

Fig. 2. Simulation setup for parameter estimation of diesel genset model.

A resistive load of 50% of the generator capacity (Load1) is always connected as a base load. The generator is excited with different perturbation power of around 10% of total

TABLE I
SYNCHRONOUS MACHINE, DEGOV, AND DC4B MODEL PARAMETERS

Governor Parameters	**Value(s)**
Controller Constants (T_1, T_2, T_3) [s]	1e−4, 0, 0.2242
Governor Time Constants (T_4, T_5, T_6) [s]	0.25, 0, 5.74e−3
Gain (K)	50
Engine Time Delay (T_d) [s]	1.67e−2
Exciter Parameters	**Value(s)**
Low-pass Filter Time Constant (T_r) [s]	0.002
Voltage Regulator Gain and Time Constant (K_a, T_a [s])	1, 0.02
Voltage Regulator Output Limits ($V_{r_{min}}$, $V_{r_{max}}$)	0, 8
Damping Filter (K_f, T_f [s])	0, 1
Exciter Gain and Time Constant (K_e, T_e [s])	1, 0.02
PID Settings (K_p, K_i, K_d, N_d, K_b)	20, 100, 1, 10000, 5

generator capacity (Load2). The perturbation signal is a square wave signal that gives various step changes in active power. Thus, two loads of 200 kW (Load 1) and 40 kW (Load 2) are connected to the given system. The resulting frequency changes are measured through a phase-locked-loop (PLL). Because the online measurements of frequency are more likely to contain noise in a real system, additional noise is added to input measurements to make it realistic. The performance of MHE is tested and evaluated with non-Gaussian noise in the frequency and power measurements. PLL measurements have typical noise covariance of 10^{-7} [25], thus an signal-to-noise (SNR) ratio of 65 dB is added to the frequency measurements in the model. The skewness and kurtosis values for the non-Gaussian noise are set to 0.5 and 7.0. The typical values of skewness and kurtosis have been chosen based on [26]. The change in electrical power is computed by measuring the generator terminal voltage v_{abc} and the output current i_{abc}. The noisy measurements of frequency and electrical power are fed to the inputs of MHE as mentioned in Section III.

At each sampling instant, the MHE uses frequency measurements to estimate the multiple parameters (a_{12}, a_{21}, a_{22}) of the linearized diesel genset model. The convergence time, (T_c) is the product of horizon length (L) and sampling time (T_s) of MHE given by: $T_c = L \times T_s$.

We are taking $L = 700$ and $T_s = 0.003$ s to capture the 2.1 s period of the excitation signal. Smaller values of L created larger deviations and did not provide ample estimates [12]. A larger horizon length was chosen because of the noisy measurements and completely unknown set of parameters. The sampling time of MHE was selected based on the larger real part of eigenvalue from the system matrix. The sampling time will be at least 10–20 times smaller than the calculated time constant from the eigenvalue [27]. More details regarding the MHE algorithm and implementation are available in [13].

V. RESULTS AND ANALYSIS

The estimator performance is analysed based on the non-Gaussian noisy measurements and varying the inertial range of values in the given DG system. Initially, inertia in the detailed Simulink model was set to 0.388 s. However, the inertial value along with all other parameters of the simplified model inside MHE is assumed to be unknown while performing the estimation. MHE takes the minimum value of the constraint limit, 0 as the initial guess of each parameter. It collects 700 data points to converge and provide the first estimate of the state variable and parameters for the given linear model. In this paper, we focus on investigating the accuracy of the developed simplified frequency dynamics model using the parameters estimated by MHE. For $M = 0.388$ s, the estimation results are shown in Fig. 3.

A. State and Input Power Estimation

MHE estimates the frequency as shown in Figure 3(d) for the case. Additionally, MHE estimates the input power supplied by the generator at the same time shown in Figure 3(e). Even in the presence of non-Gaussian noisy measurements, MHE converges within a short time period of 2.1 s. The accuracy in the estimation is illustrated by calculating the normalized root mean square error (NRMSE) between MHE estimates and the true values (without noise). The root mean square error (RMSE) for the frequency and input measurements were normalized by taking the difference between the maximum and minimum value of the observations to calculate NRMSE given by (9) below:

$$\text{NRMSE} = \frac{\sqrt{\frac{1}{n}\Sigma_{i=1}^{n}\left(x_i - \hat{x_i}\right)^2}}{\max(x_i) - \min(x_i)} \tag{9}$$

where, n represents the total number of data points, x_i represents the true values of inputs (ω and P_e) and $\hat{x_i}$ represents the estimated values of ω and P_e. Once the MHE converges, the NRMSE calculation is performed. MHE performance was tested for different inertia values varying from M_1 to $5M_1$. For all the cases, the estimator tracks the input measurements very accurately as illustrated in Table II. The estimation of frequency and input power is performed with an NRMSE value less than 5% which is an acceptable range for the power system dynamic studies and controller design (MHE also performed well under the Gaussian noise distribution, but the results are not shown due to space limitations).

TABLE II
PERFORMANCE METRIC ANALYSIS

Inertia	NRMSE (%)		CoV (%)		
(M_1 = 0.388 s)	ω	P_e	a_{12}	a_{21}	a_{22}
M_1	0.665	3.159	0.678	1.997	2.240
$2M_1$	0.581	3.106	0.521	0.873	1.047
$3M_1$	0.576	3.115	0.972	0.928	0.944
$4M_1$	0.557	3.103	0.98	1.056	1.005
$5M_1$	0.514	3.093	0.906	1.198	1.04

B. Estimation of Parameters

MHE estimates the parameters of the linear model sufficient enough to represent the frequency dynamics based on the input measurements from PLL and generator. The average estimates of the parameters a_{12}, a_{21}, and a_{22} were found to be 48.67,

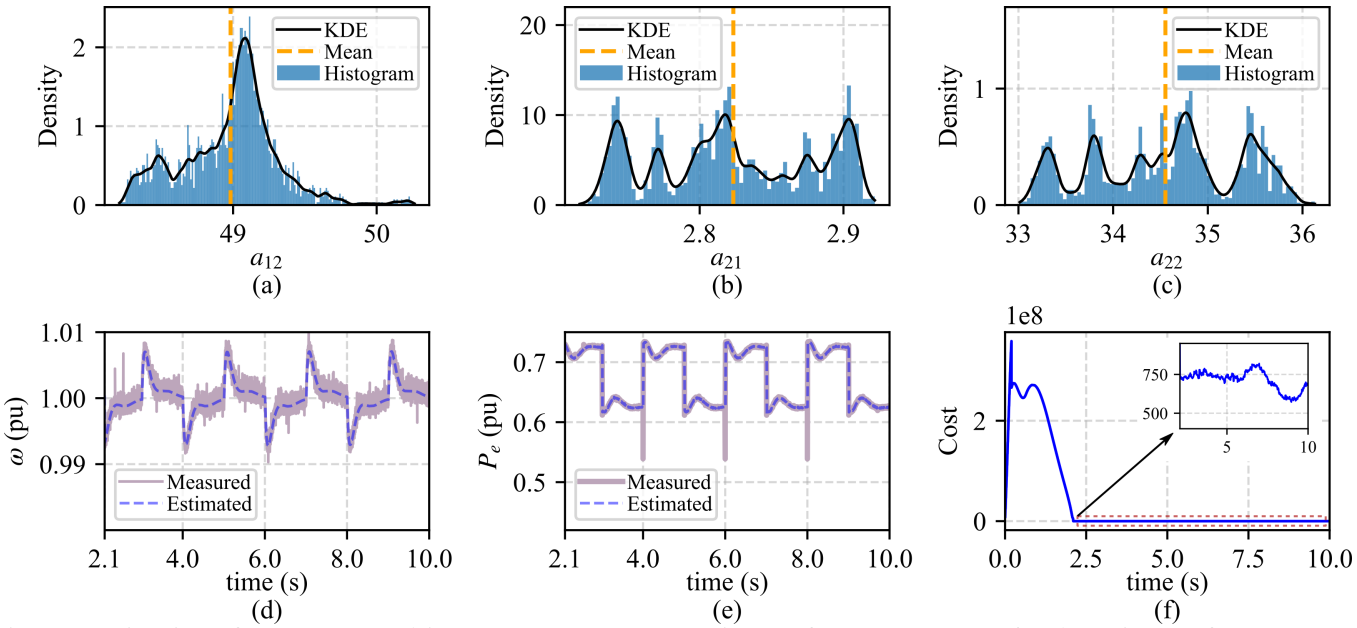

Fig. 3. Estimation of parameters and input measurements. a) estimate of a_{12} (mean = 48.67), b) estimate of a_{21} (mean = 2.84), c) estimate of a_{22} (mean = 34.63), d) estimation of frequency, e) estimation of electrical power, and f) plot of the cost function. The magnified portion on the top right corner shows the cost function is not exactly zero after convergence because of the noise.

2.84, and 34.63 which are represented by the yellow dashed line in Figures 3(a) – (c). The estimated parametric results are analyzed by plotting a histogram and kernel density estimate (KDE) for each of the parameters. The non-Gaussian noisy measurement distribution may not give an exactly normally distributed estimates as seen from the KDE plots. However, the data points in each of the estimates in the KDE plots are concentrated around the same range of values. For a small change in frequency and input power, the parameters do not change significantly which means the parameters' values should remain in a constant range. This is clearly seen in the histogram and KDE plots as well. The percentage coefficient of variation (CoV) is calculated for the estimated parameters by dividing the standard deviation (σ) with the mean value (μ) i.e. CoV $= \frac{\sigma}{\mu}$. The CoV values show the extent of the variability in the estimated data.

The calculated CoV values of the estimates for varying M values (from M_1 to $5M_1$) presented in Table II which are less than 10% showing a low variance in the estimation. Thus, MHE is able to extract all the parameters efficiently in the presence of non-Gaussian noise and without the knowledge of any parameter values in the linearized system model for wide range of inertial variation. Figure 3 (f) shows the optimization cost function plot to calculate optimum parameters along with the state variable. MHE tries to achieve a minimum cost function defined over a finite horizon length. Initially, the cost function is seen to be reaching a higher value. However, once the measurements are collected over the finite horizon length, the cost function gets to a minimum value as shown in the magnified portion of the plot shown in Figure 3 (f). The cost function does not completely hit zero due to the noise in the measurements.

C. Validation of Parameter Estimates

MHE works well in estimating the state and parameters with significantly small error. However, validating the estimated parameter is an important step to check how accurately it captures the frequency response in comparison with the detailed model. It can be achieved by using the estimated parameters back in the simplified model. During this process, we used the electrical power P_e as an input to the model with the varying loading conditions as shown in Figure 4 (a). Initially, the base load was set to 80 kW and then loads were increased by 0.2 pu at every 2 s and started decreasing by same amount after $t = 8$ s. If the frequency response from the simplified model and detailed simulation setup match, it can be said that the derived model is accurate enough for future application in predictive controller design. In this experiment, the results of frequency we obtained from the simplified model using MHE estimates and from PLL are shown in Fig. 4 (b) which shows that both of the responses are quite close. The NRMSE was calculated and found to be 3.17% which reflects a very high accuracy.

VI. Conclusions

The objective of this paper was to develop a simplified frequency dynamics model of a diesel genset based on a detailed Simulink diesel genset system and simultaneously estimate all unknown parameters of the simplified model using an optimization-based MHE algorithm for dynamic microgrid simulation. A non-intrusive square wave signal was used to perturb the system frequency dynamics while avoiding system imbalance. The proposed approach provided the online estimation of all parameters for the given non-linear problem with constraints on the model estimates. Even under typical noisy

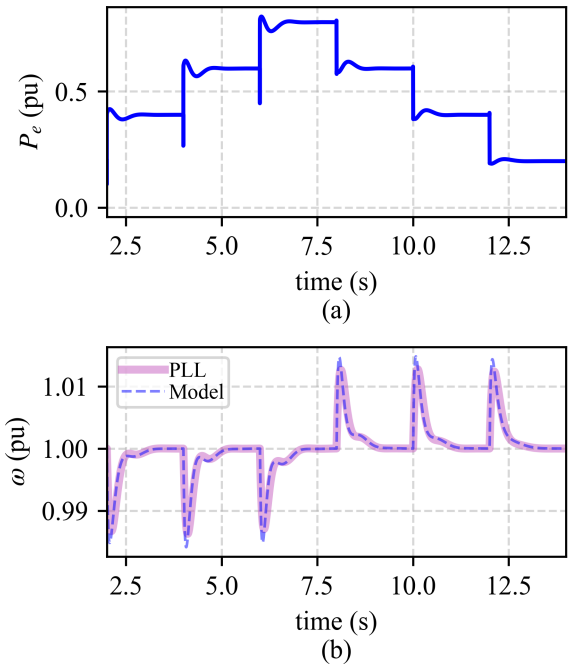

Fig. 4. Parameters verification (a) Electrical power input measured from V_{abc} and I_{abc} of DG (b) Plot of frequency from PLL measurements and simplified model using estimated parameters.

PLL measurements, MHE accurately estimated the parameters and states which was verified by the comparing PLL frequency with the frequency response from simplified model whose parameters are the estimates of MHE. The proposed state-of-the-art algorithm quickly converges and the parameters of the model were validated with a minimum NRMSE of 3.17% . The developed simplified model with the proposed estimation technique will be conducive for accurate modeling and proper controller design of renewable integrated diesel generator system with time-varying parameters.

VII. Acknowledgment

The author would like to thank Dr. Hyungjin Choi from Sandia National Laboratories for the technical review of this paper.

References

[1] "Theoretical study of di diesel engine performance and pollutant emissions using comparable air-side and fuel-side oxygen addition," *Energy Conversion and Management*, vol. 48, no. 11, pp. 2962–2970, 2007.

[2] S. Pelland, D. Turcotte, G. Colgate, and A. Swingler, "Nemiah valley photovoltaic-diesel mini-grid: System performance and fuel saving based on one year of monitored data," *IEEE Transactions on Sustainable Energy*, vol. 3, no. 1, pp. 167–175, 2012.

[3] "ACEP – alaska center for energy & power," *Alaska Center for Energy and Power (ACEP)*. [Online]. Available: https://acep.uaf.edu/

[4] G. Venkataramanan and Bingsen Wang, "Dynamic modeling and control of three phase pulse width modulated power converters using phasors," in *IEEE* 35^{th} *Annual Power Electronics Specialists Conference*, June 2004, pp. 2822–2828.

[5] F. D. de Mello and L. Hannett, "Validation of synchronous machine models and derivation of model parameters from tests," *IEEE Transactions on Power Apparatus and Systems*, vol. PAS-100, pp. 662–672, 1981.

[6] T. Hosseinalizadeh, S. M. Salamati, S. A. Salamati, and G. B. Gharehpetian, "Improvement of identification procedure using hybrid cuckoo search algorithm for turbine-governor and excitation system," *IEEE Transactions on Energy Conversion*, vol. 34, no. 2, pp. 585–593, 2019.

[7] Q. Long, H. Yu, F. Xie, N. Lu, and D. Lubkeman, "Diesel generator model parameterization for microgrid simulation using hybrid box-constrained levenberg-marquardt algorithm," *IEEE Transactions on Smart Grid*, p. 1–1, 2020. [Online]. Available: http://dx.doi.org/10.1109/TSG.2020.3026617

[8] T. Inoue, H. Taniguchi, Y. Ikeguchi, and K. Yoshida, "Estimation of power system inertia constant and capacity of spinning-reserve support generators using measured frequency transients," *IEEE Transactions on Power Systems*, vol. 12, no. 1, pp. 136–143, 1997.

[9] C. Trudinger, M. Raupach, P. Rayner, and I. Enting, "Using the kalman filter for parameter estimation in biogeochemical models," *Environmetrics*, vol. 19, pp. 849 – 870, 12 2008.

[10] G. Marafioti, S. Tebbani, D. Beauvois, G. Becerra, A. Isambert, and M. Hovd, "Unscented kalman filter state and parameter estimation in a photobioreactor for microalgae production," *IFAC Proceedings Volumes*, vol. 42, no. 11, pp. 804 – 809, 2009, 7th IFAC Symposium on Advanced Control of Chemical Processes.

[11] E. L. Haseltine and J. B. Rawlings, "Critical evaluation of extended kalman filtering and moving-horizon estimation," *Industrial & Engineering Chemistry Research*, vol. 44, no. 8, pp. 2451–2460, 2005. [Online]. Available: https://doi.org/10.1021/ie0343081

[12] J. B. Rawlings, D. Q. Mayne, and M. M. Diehl, *Model predictive control theory, computation, and design*. Nob Hill Publishing, 2017.

[13] U. Tamrakar, "Optimization-based fast-frequency support in low inertia power systems," Ph.D. dissertation, South Dakota State University, 2020.

[14] M. Rauniyar, S. Berg, S. Subedi, T. M. Hansen, R. Fourney, R. Tonkoski, and U. Tamrakar, "Evaluation of probing signals for implementing moving horizon inertia estimation in microgrids," in *2020 52nd North American Power Symposium (NAPS)*, 2021, pp. 1–6.

[15] P. Kundur, N. J. Balu, and M. G. Lauby, *Power system stability and control*. McGraw-Hill New York, 1994, vol. 7.

[16] H. J. Ferreau, T. Kraus, M. Vukov, W. Saeys, and M. Diehl, "High-speed moving horizon estimation based on automatic code generation," in *2012 IEEE 51st IEEE Conference on Decision and Control (CDC)*, 2012, pp. 687–692.

[17] P. Kühl, M. Diehl, T. Kraus, J. P. Schlöder, and H. G. Bock, "A real-time algorithm for moving horizon state and parameter estimation," *Computers and Chemical Engineering*, vol. 35, no. 1, pp. 71–83, 2011.

[18] J. A. Andersson, J. Gillis, G. Horn, J. B. Rawlings, and M. Diehl, "CasADi: a software framework for nonlinear optimization and optimal control," *Mathematical Programming Computation*, vol. 11, no. 1, 2019. [Online]. Available: https://doi.org/10.1007/s12532-018-0139-4

[19] Mathworks, "Synchronous machine," https://www.mathworks.com/help/physmod/sps/powersys/ref/synchronousmachine.html, 2020.

[20] PowerWorld Corporation, "Governor DEGOV," https://www.powerworld.com/WebHelp/Content/TransientModels_HTML/Governor\%20DEGOV.html, 2020.

[21] B. Lundstrom, P. Koralewicz, B. Miller, J. Fossum, S. Truitt, and J. Wang, "Considerations for microgrid co-design: Performance verification approach, metrics, and interoperability," https://www.nrel.gov/docs/fy21osti/78143.pdf, 10 2020, nREL/PR-5D00-78143.

[22] PowerWorld Corporation, "Exciter DC4B and ESDC4B," https://www.powerworld.com/WebHelp/Content/TransientModels_HTML/Exciter\%20DC4B\%20and\%20ESDC4B.htm, 2020.

[23] "Approved IEEE Recommended Practice for Excitation Systems for Power Stability Studies (Superseded by 421.5-2005)," *IEEE Std P421.5/D15*, 2005.

[24] Mathworks, "DC1A Excitation System," https://www.mathworks.com/help/physmod/sps/powersys/ref/dc1aexcitationsystem.html, 2020.

[25] H. Karimi, M. Karimi-Ghartemani, and M. R. Iravani, "Estimation of frequency and its rate of change for applications in power systems," *IEEE Transactions on Power Delivery*, vol. 19, no. 2, pp. 472–480, 2004.

[26] S. Wang, J. Zhao, Z. Huang, and R. Diao, "Assessing gaussian assumption of PMU measurement error using field data," *IEEE Transactions on Power Delivery*, vol. 33, no. 6, pp. 3233–3236, 2017.

[27] G. A. Perdikaris, *Discrete-Time Systems*. Dordrecht: Springer Netherlands, 1991, pp. 139–234. [Online]. Available: https://doi.org/10.1007/978-94-015-7929-2_3